Surface electronic structure of Re(0001): A spin-resolved photoemission study

Marcel Holtmann,[1,*] Peter Krüger,[2] Koji Miyamoto,[3] Taichi Okuda,[3] Kenya Shimada,[3] and Markus Donath[1,†]

[1]*Physikalisches Institut, University of Münster, Wilhelm-Klemm-Straße 10, 48149 Münster, Germany*

[2]*Institut für Festkörpertheorie, University of Münster, Wilhelm-Klemm-Straße 10, 48149 Münster, Germany*

[3]*Hiroshima Synchrotron Radiation Center, Hiroshima University, 2-313 Kagamiyama, Higashi-Hiroshima 739-0046, Japan*

(Received 27 January 2023; revised 8 March 2023; accepted 5 April 2023; published 26 April 2023)

The surface electronic structure of Re(0001) has been investigated in a combined experimental and theoretical study. Spin- and angle-resolved photoemission was employed to unravel the spin-dependent $E(\mathbf{k}_\parallel)$ dispersion of electronic states along the $\overline{\Gamma}\,\overline{\mathrm{M}}$ and $\overline{\Gamma}\,\overline{\mathrm{K}}$ directions. The results are compared with band-structure calculations based on density-functional theory. Additional calculations include transitions into final states by taking into account the corresponding matrix elements. Recently, Shockley- and Tamm-type surface states close to E_F were identified, which were found to be mixed by spin-orbit coupling. Here, we determined the Rashba parameter α_R of the surface state around $\overline{\Gamma}$ to 0.32 and 0.34 eV Å along $\overline{\Gamma}\,\overline{\mathrm{M}}$ and $\overline{\Gamma}\,\overline{\mathrm{K}}$, respectively. Furthermore, we extend our analysis to a wider $E(\mathbf{k}_\parallel)$ range revealing a multitude of electronic states along both high-symmetry directions. In particular, Rashba-type spin splittings are observed around the high-symmetry $\overline{\Gamma}$ and $\overline{\mathrm{M}}$ points. At variance with theoretical predictions for a perfect hcp(0001) surface, we do not find any out-of-plane spin polarization. This is caused by monatomic steps of a real Re(0001) surface with alternating terminations, leading on average to an effective sixfold surface symmetry and vanishing net out-of-plane spin polarization.

DOI: 10.1103/PhysRevB.107.165420

I. INTRODUCTION

Electronic states at surfaces of high-Z materials continue to attract scientific interest because the broken inversion symmetry at the surface combined with spin-orbit coupling (SOC) results in spin-momentum locking. Examples of heavy metals with remarkable spin-orbit-induced effects include the Au(111) surface, where the prototypical L-gap Shockley state exhibits a Rashba-type spin splitting [1–4], and the W(110) surface, which hosts a topologically protected Dirac-like state in a SOC-induced symmetry gap [5,6]. Spin-momentum-locked surface states might be of interest for future spintronics devices, in particular if they are located close to the Fermi level. Therefore, high-Z transition metals with high density of d-type states at the Fermi level such as rhenium are prototypical materials of interest.

Compared with gold or tungsten, much less is known about rhenium. Calculations of the bulk electronic structure and Fermi surface of rhenium were performed by Mattheiss [7]. Recent slab calculations for the Re(0001) surface revealed a wealth of surface states and resonances and predict SOC-induced spin splittings [8]. Early photoemission experiments on Re(0001) found two surface-derived features at $\overline{\Gamma}$ within 2 eV below the Fermi level [9]. The existence of an unoccupied surface state around $\overline{\Gamma}$ with negative parabolic dispersion was deduced from the observation of standing waves in scanning tunneling spectroscopy experiments [10]. Further examination of the electronic structure of Re(0001) was conducted by spin-resolved time-of-flight momentum microscopy and scanning tunneling spectroscopy [11,12]. Using spin-resolved inverse photoemission, the unoccupied part of the surface state around $\overline{\Gamma}$ was investigated with focus on the spin polarization [13]. A comprehensive study of the unoccupied electronic structure of Re(0001) with a particular focus on the Rashba-type spin splitting of the image potential state is provided in Ref. [14]. Recently, it has been discovered that the Re(0001) surface hosts Shockley- and Tamm-type surface states in different kinds of energy gaps [15]. These states are found to be mixed by SOC in a certain wave-vector range, forming a W-shaped $E(\mathbf{k}_\parallel)$ dispersion. As a consequence, the resulting band consists of two electron pockets and one hole pocket, crossing the Fermi energy four times.

The goal of this report is to extend the knowledge on the occupied electronic structure of Re(0001). We present a comprehensive spin-resolved photoemission study along the $\overline{\Gamma}\,\overline{\mathrm{K}}$ and $\overline{\Gamma}\,\overline{\mathrm{M}}$ directions. Our experimental results are complemented by density-functional theory (DFT) calculations of the spin-dependent electronic structure. In addition, we present calculations, which include transitions into final states by taking into account the corresponding matrix elements. The latter method is of particular importance to elucidate the origin of the experimentally observed spin polarization.

II. EXPERIMENTAL DETAILS

We performed (spin- and) angle-resolved photoemission [(S)ARPES] measurements at the BL-9B end station of the Hiroshima Synchrotron Radiation Center (HiSOR), while preliminary data (not shown here) had been taken at BL-1. We used linearly polarized photons with energies between

*marcel.holtmann@uni-muenster.de

†markus.donath@uni-muenster.de

 ©2023 American Physical Society

$\hbar\omega = 24$ eV and 72 eV. The photon-energy-dependent ARPES data show that most of the observed spectral features are surface related because they do not change their energy vs momentum dispersion upon varying photon energy [16]. In this report we will present data for $\hbar\omega = 24$ eV because the intensities of surface-derived features are pronounced for this energy. The emitted photoelectrons were detected using a hemispherical energy analyzer (VG-Scienta R4000), whose lens axis is fixed at an angle of 50° with respect to the incident light beam. Three-dimensional spin-polarization analysis is provided by the ESPRESSO machine [17,18], that is based on VLEED (very low-energy electron diffraction)-type spin-polarization detection. During our measurement, the Sherman function was $S = 0.28$. The energy resolution for ARPES and SARPES was 25 and 50 meV, respectively, and the angular resolution was $\leqslant 1°$. The base pressure in the ultrahigh-vacuum (UHV) system was better than 1×10^{-10} mbar. The sample was kept below $T = 45$ K during the measurements.

The Re(0001) sample from MaTecK GmbH (Germany) was cleaned by cycles of annealing at 1400 K in oxygen atmosphere ($p = 5 \times 10^{-8}$ mbar), followed by a short flash to 1800 K [10,13]. A small to vanishing carbon signal in Auger-electron spectra and a sharp hexagonal low-energy electron diffraction (LEED) pattern served as criteria for a clean and well-ordered surface. An ideal hcp(0001) surface consists of layers with hexagonal atomic symmetry with an A-B-type stacking order. This results in a threefold symmetry. The surface of a real single crystal, however, usually consists of flat terraces separated by monatomic steps [10]. This leads to surface terminations with A- as well as B-type layers. If the spot size of the photon beam in (S)ARPES experiments is large compared with the dimensions of the step terraces, the measurement averages over both surface terminations leading to an effective sixfold surface symmetry [19].

III. THEORETICAL DETAILS

The structural and electronic properties have been calculated within the local-density approximation [20] of DFT. Norm-conserving pseudopotentials in separable form [21,22] that include scalar relativistic corrections and SOC [23,24] have been used. For the representation of the wave functions, we employ a basis of atom-centered Gaussian orbitals. We use different shells of s-, p-, d- and s^*-type orbitals and decay constants of 0.10, 0.35, and 1.07 (in atomic units) for each type. The Re(0001) surface is treated within the supercell approach by employing a slab of 40 Re layers. A vacuum region of 22 Å is utilized to decouple neighboring slabs. Brillouin-zone integrations are carried out using a $12 \times 12 \times 1$ Monkhorst-Pack mesh [25]. Relaxations of the topmost eight layers have been taken into account. Details of the resulting structural properties are given in Ref. [13].

We simulate the photoemission process by assuming a plane wave with the respective spin orientation as the final state and compute the dipole transition matrix elements for a light incidence angle of 50° by employing the initial states resulting from our DFT calculation. An exponential damping term with a decay length of 1.25 Å has been used to consider the finite escape depth of the outgoing electrons. To take the simultaneous existence of A- and B- type layers into account, the intensity of the photocurrent has been determined as average resulting from calculations for two slabs which are rotated by 180° with respect to each other.

IV. RESULTS AND DISCUSSION

A. Electronic states along $\overline{\Gamma}\,\overline{\mathrm{M}}$

1. *Electronic states around* $\overline{\Gamma}$

Our (S)ARPES results for the electronic states in $\overline{\Gamma}\,\overline{\mathrm{M}}$ direction around $\overline{\Gamma}$ are shown in Fig. 1. Figure 1(a) presents the second derivative of the ARPES intensity as a contour plot for p-polarized photons with an energy of $\hbar\omega = 24$ eV.[1] The intensity is given on a linear color scale (brown-yellow-green-blue) and distinct features are labeled by Greek letters α to η. The black lines indicate "pathways" of energy distribution curves (EDCs) for given electron emission angles θ. For the marked angles, SARPES spectra with sensitivity to the Rashba spin-polarization component have been obtained, as shown in Fig. 1(b). The geometry is displayed in the inset at the top right of the figure. The spin-up (spin-down) character of detected photoelectrons is indicated by red (blue) dots. The left (right) column of Fig. 1(b) features spectra taken for negative (positive) electron emission angles. Spectra for opposite angles with respect to $\theta = 0°$, corresponding to $\overline{\Gamma}$, are horizontally aligned to each other. Due to the effective sixfold symmetry of the surface, the electronic states are expected to be symmetric for positive and negative $\mathbf{k}_\parallel$, implying that $\overline{\Gamma}\,\overline{\mathrm{M}'}$ is equivalent to $\overline{\Gamma}\,\overline{\mathrm{M}}$. However, the photon incidence angle of 50° breaks the symmetry of the experiment. Therefore, the spectral intensities may differ for positive and negative θ.

In Fig. 1(a), the electron pockets of the W-shaped surface state are reflected by the α, β, and γ features. As discussed in Ref. [15], the intensity of α is rather weak due to transitions into final states. In addition, a band doublet labeled δ crosses the Fermi energy at about ± 0.5 Å^{-1}. The features ϵ, ζ, and η appear at higher binding energies, with η representing another band doublet.

The spin-resolved spectra in Fig. 1(b) prove the Rashba-type behavior of the spin polarization for α and β [15]: α is predominantly populated by spin-up electrons for negative angles and spin-down electrons for positive angles. The opposite holds true for β. The spin polarization of the γ branch is apparent from the spectra for $\theta = \pm 9.5°$, where γ is dominated by red (blue) intensity for negative (positive) angles. The band doublet δ shows high intensity for spin-down (spin-up) photoelectrons at negative (positive) electron emission angles. Concerning the features at higher binding energies, ϵ does not show a clear spin polarization. ζ appears at about $E - E_\mathrm{F} = -1.1$ eV in the spectrum for $\theta = 15.5°$ as a predominantly blue signal. The doublet η is identified in the spectrum for $\theta = -11.5°$ ($\theta = +11.5°$) as the red-blue (blue-red) feature at energies of about -1.1 and -1.3 eV.

Since the $\overline{\Gamma}\,\overline{\mathrm{M}}$ direction coincides with a mirror plane of the Re(0001) surface, out-of-plane spin polarization is forbidden for symmetry reasons. We measured spin-resolved

[1]We note that the surface-derived features are suppressed in ARPES data with s-polarized light.

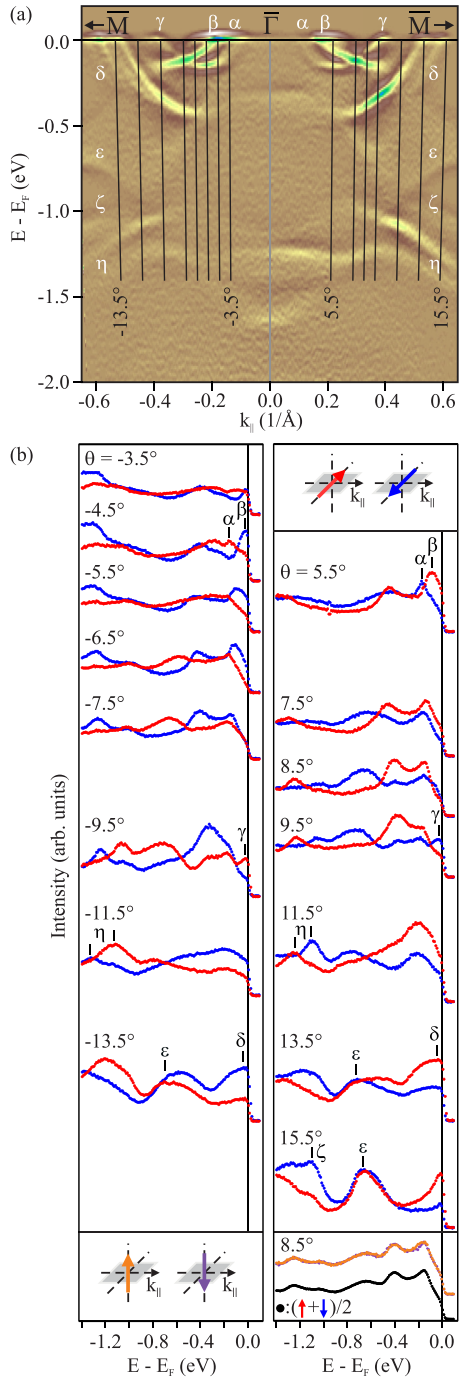

FIG. 1. (S)ARPES data for Re(0001) using *p*-polarized light of $\hbar\omega = 24$ eV. (a) Contour plot of ARPES intensity for $E(\mathbf{k}_\parallel)$ along $\overline{\Gamma}\,\overline{\mathrm{M}}$ (second derivative). (b) Spin-resolved spectra (Rashba component in red and blue, spin-averaged Rashba component in black, out-of-plane component in orange and purple) for selected electron emission angles θ [marked by black lines in panel (a)]. The Greek letters are used to label spectral features.

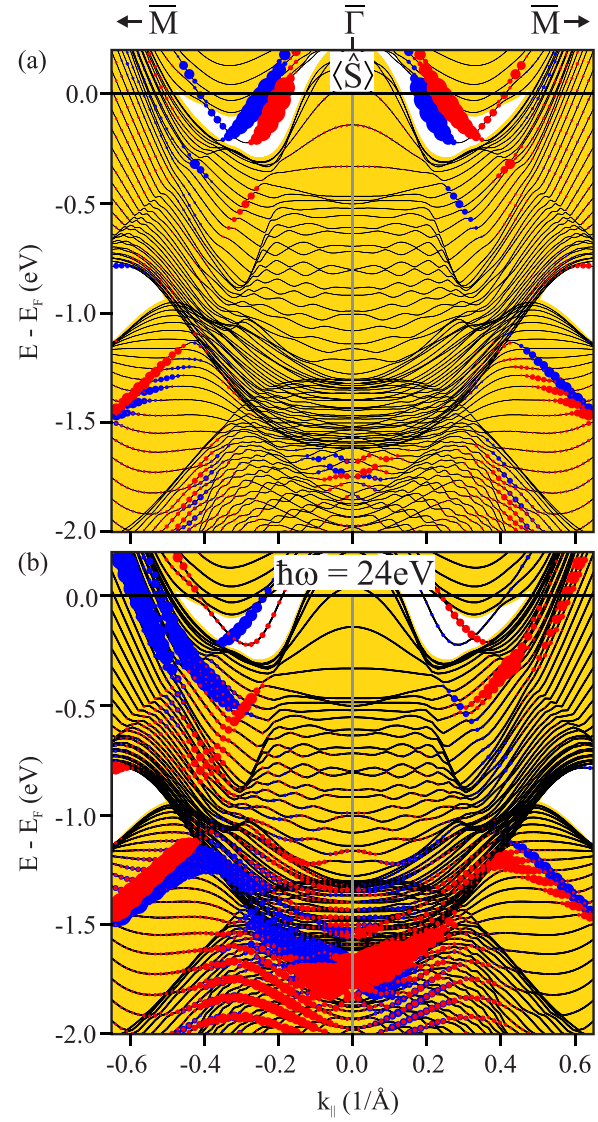

FIG. 2. DFT calculations of the Re(0001) surface along $\overline{\Gamma}\,\overline{\mathrm{M}}$. The surface-projected bulk band structure is indicated by golden-shaded areas. Red (blue) dots in panel (a) indicate the intrinsic spin expectation value $\langle\hat{S}\rangle$ regarding the Rashba component for spin-up (spin-down) electrons of the surface states. (b) Calculations including transition matrix elements using free-electron-like final states and $\hbar\omega = 24$ eV. The dot size is a measure of the expected spectral intensity in the SARPES experiment. Note that red dots are drawn on top of blue dots.

spectra sensitive to the out-of-plane component for $\theta = 8.5°$, as shown in the lower part of Fig. 1(b)—color coded in orange and purple. As theoretically expected, there is no out-of-plane spin polarization.

Figure 2 shows our theoretical results based on DFT including SOC of the Re(0001) surface along the $\overline{\Gamma}\,\overline{\mathrm{M}}$ direction. The chosen $E(\mathbf{k}_\parallel)$ region matches that of the ARPES data in Fig. 1(a). The surface-projected bulk band structure is represented by the golden-shaded areas, the black lines indicate the bands of the slab calculation. The spin information with regard to the Rashba component, represented by blue and red dots, differs in Figs. 2(a) and 2(b): In Fig. 2(a), the spin expectation value $\langle\hat{S}\rangle$ is displayed for spin-up (red) and spin-down (blue) electrons, which is intrinsic to the surface states (*initial states*). In Fig. 2(b), the dot size is a measure of the expected spectral intensity in the SARPES experiment,

thereby modeling the experimental results. The calculation includes transition matrix elements using free-electron-like *final states* for $\hbar\omega = 24$ eV.

A comparison between theory and experiment in Figs. 2(a) and 1(a) shows good overall agreement concerning the $E(\mathbf{k}_\parallel)$ dispersion. According to Fig. 2(a), the features δ, ϵ, and ζ appear in regions of high density of states. A more detailed analysis showed that δ is a surface-derived band, while ϵ and ζ mark band-gap boundaries. α, β, γ, and η, on the other hand, stand out by their nonzero spin expectation value, characteristic for surface-related bands. η is interpreted as a surface resonance, since it overlaps with bulk bands.

At variance with the agreement described above, the sign of $\langle\hat{S}\rangle$ in Fig. 2(a) for γ does not match that in the SARPES data in Fig. 1(b). Therefore, we performed additional DFT calculations including final-state effects by taking into account the transition matrix elements, which are presented in Fig. 2(b). In the results of these calculations, the sign of the spin polarization of γ is reversed compared with the intrinsic spin expectation value. We conclude that the experimentally observed spin polarization is a consequence of transitions into final states in SARPES [26].

Furthermore, the DFT calculations including transitions into final states in Fig. 2(b) enable us to evaluate spectral intensities. The low intensity of α compared with β is now well described by theory, as well as the high spectral intensity of δ, as seen in both the ARPES contour plot and the spin-resolved EDCs.

2. *Electronic states around* $\overline{\mathrm{M}}$

Figures 3(a) and 3(b) show ARPES and SARPES measurements along $\overline{\Gamma}\,\overline{\mathrm{M}}$ for $\mathbf{k}_\parallel$ values centered around the $\overline{\mathrm{M}}$ point. For these measurements, the sample had to be rotated with respect to the light incidence angle. Therefore, the spectral intensities cannot be directly compared between Figs. 1(a) and 3(a). In addition, the color scales are not calibrated between the two plots. Otherwise, the presentation of the data is equivalent to Fig. 1. The $\mathbf{k}_\parallel$ range is chosen in such a way that the range used in Fig. 1(a) is continued here. The white line marks the "experimental horizon", which is given by the maximum angle that was measured. The spectra in Fig. 3(b) are separated into two columns again. Here, the right-hand (left-hand) column contains the spectra for $\mathbf{k}_\parallel$ values lower (higher) than the $\overline{\mathrm{M}}$ point.

In Fig. 3(a), the $E(\mathbf{k}_\parallel)$ dispersion of the features ϵ, ζ, and η from Fig. 1(a) finds continuation for larger $\mathbf{k}_\parallel$ values. ϵ splits into a band doublet which is bent upwards and crosses the Fermi energy at about $\mathbf{k}_\parallel = -1.0$ Å^{-1}. ϵ' denotes the same band in the second Brillouin zone. Two bands stand out crossing the $\overline{\mathrm{M}}$ point at energies $E - E_\mathrm{F} \approx -0.6$ eV (κ) and $E - E_\mathrm{F} \approx -1.6$ eV (λ).

In the spin-resolved spectra of Fig. 3(b) all features ϵ, ϵ', ζ, η, κ, and λ are clearly resolved. The band doublet ϵ shows a complex behavior: Each partial spin spectrum contains more than one spectral component with different spin-up and spin-down intensities. In addition, the spin polarization is not clearly reversed for ϵ', which would have been expected for a simple Rashba-type behavior. The dominant spectral feature κ does not show any spin splitting close to $\overline{\mathrm{M}}$. Further away from $\overline{\mathrm{M}}$, however, where hybridization with other states comes into play, κ shows a Rashba-type spin splitting (compare spectra for $\theta = -50°$ and $-25°$). The rather flat spectral feature λ exhibits a small, but significant Rashba-type spin splitting with reversed sign compared with κ.

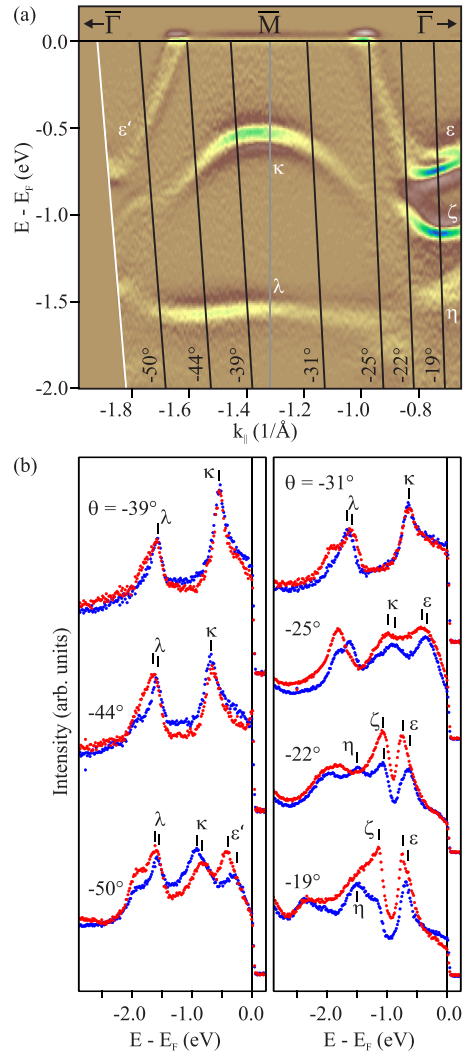

FIG. 3. (S)ARPES data for Re(0001) using p-polarized light of $\hbar\omega = 24$ eV for $\mathbf{k}_\parallel$ values centered around the $\overline{\mathrm{M}}$ point. (a) Contour plot of ARPES intensity for $E(\mathbf{k}_\parallel)$ along $\overline{\Gamma}\,\overline{\mathrm{M}}$ (second derivative). (b) Spin-resolved spectra, sensitive to the Rashba component, for selected electron emission angles θ [marked by black lines in panel (a)]. The Greek letters are used to label features in both plots.

To interpret the observed experimental results, we again compare them with DFT calculations, which are shown in Fig. 4(a). The figure is presented in the same way as Fig. 2(a). We identify the band doublet ϵ as a band-edge state with a spin-polarized surface component within the gap. The spin behavior is reversed for ϵ', which seems to be at variance with the experimental results. ζ is a band-edge state with small spin polarization, in agreement with the SARPES data. κ is attributed to a region of high bulk state density around $\overline{\mathrm{M}}$ with no spin polarization, as observed in the experiment. η is identified as a surface resonance, which transitions into λ close to $\overline{\mathrm{M}}$, both with small spin polarization. λ exhibits a Rashba-type spin polarization in theory and experiment.

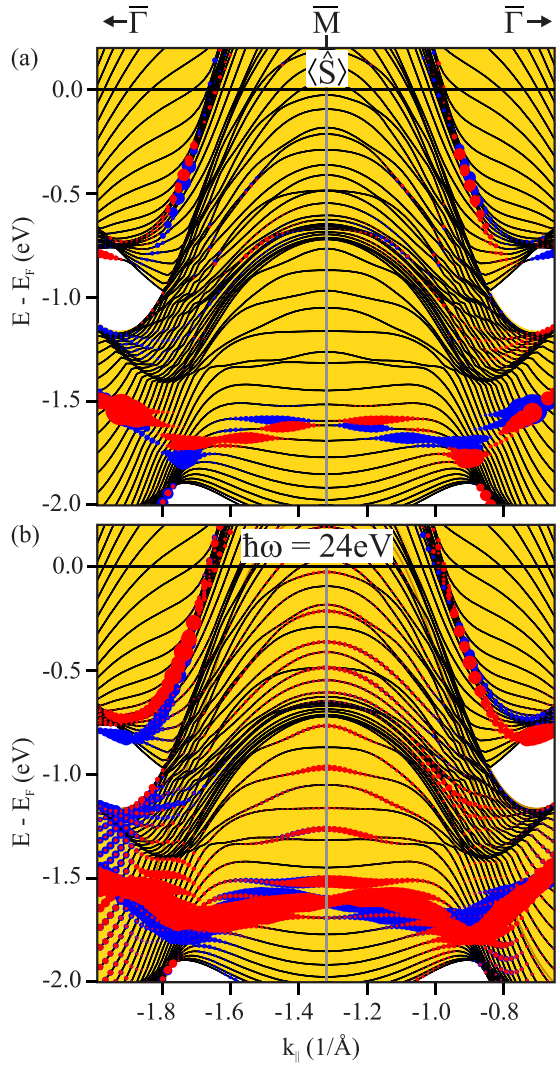

FIG. 4. DFT calculations of the Re(0001) surface along $\overline{\Gamma}\,\overline{\mathrm{M}}$ for $\mathbf{k}_\parallel$ values in the vicinity of the $\overline{\mathrm{M}}$ point. The surface-projected bulk band structure is indicated by golden-shaded areas. Red (blue) dots in panel (a) indicate the intrinsic spin expectation value $\langle\hat{S}\rangle$ regarding the Rashba component for spin-up (spin-down) electrons of the surface states. (b) Calculations including transition matrix elements using free-electron-like final states and $\hbar\omega = 24$ eV. The dot size is a measure of the expected spectral intensity in the SARPES experiment. Note that red dots were drawn on top of blue dots.

To further explore the spin behavior of ϵ and ϵ', we simulate the SARPES experiment by including transitions into final states in the calculation, as shown in Fig. 4(b). Again, ϵ' and ϵ show a reversed spin order because ϵ' is in the second Brillouin zone. However, there are two notable differences with respect to the initial-state calculation: The spin polarization of the surface component has a reversed sign and the band-edge component shows a spin polarization opposite to that of the surface component. Furthermore, for $\mathbf{k}_\parallel$ values approaching $\overline{\mathrm{M}}$, the surface component becomes resonant with bulk bands and the two spin-polarized ϵ components cross each other. The agreement between experiment and theory is improved for the first Brillouin zone: There is spin polarization in the bulk-derived bands and the spin order is correctly described. However, the spin order of ϵ' is not obviously reversed in experiment. We attribute this mismatch to a complex situation: (i) The spin dependence of the calculated photocurrent changes sign as a function of $\mathbf{k}_\parallel$. (ii) There are no two equivalent measured EDCs with respect to $\overline{\mathrm{M}}$. The EDCs for fixed θ "cut" the bands differently in the first and second Brillouin zone.

B. Electronic states along $\overline{\Gamma}\,\overline{\mathrm{K}}$

ARPES and SARPES measurements of Re(0001) along $\overline{\Gamma}\,\overline{\mathrm{K}}$ are displayed in Fig. 5. The presentation of the data is equivalent to Fig. 1. In the lower part of Fig. 5(b), spin-resolved spectra for the out-of-plane component (purple and orange dots) for $\theta = -5^\circ$ and 6° are presented. These spectra are compared with spin-averaged spectra for the Rashba component at the same angles (black dots).

Concerning α, β, γ, and δ, the ARPES and SARPES data along $\overline{\Gamma}\,\overline{\mathrm{K}}$ resemble the data along $\overline{\Gamma}\,\overline{\mathrm{M}}$ with two differences: γ crosses the Fermi level at higher $\mathbf{k}_\parallel$ values closer to δ and the band doublet δ is merged into a broad feature. Both effects are a consequence of the hexagonal warping of the bands, as shown previously in a constant energy contour (CEC) [15]. In Fig. 5(a), an additional spectral feature μ appears as a doublet for $|\mathbf{k}_\parallel| > 0.4$ Å^{-1}. It consists of one feature at lower binding energy, that appears in both spin channels [see, e.g., Fig. 5(b) for $\theta = 13^\circ$]. The other feature at higher binding energy is spin polarized, spin-up (spin-down) for negative (positive) angles.

While the $\overline{\Gamma}\,\overline{\mathrm{M}}$ direction coincides with a mirror plane of the Re(0001) surface, this is not the case for $\overline{\Gamma}\,\overline{\mathrm{K}}$. As a consequence, out-of-plane spin polarization is forbidden along $\overline{\Gamma}\,\overline{\mathrm{M}}$, but not for $\overline{\Gamma}\,\overline{\mathrm{K}}$. In fact, calculations of the ideal Re(0001) surface (threefold symmetry) predict out-of-plane spin polarization for bands along $\overline{\Gamma}\,\overline{\mathrm{K}}$, in particular for α and β [8]. We measured spin-resolved spectra sensitive to the out-of-plane component for $\theta = -5^\circ$ and 6°, as shown in the lower part of Fig. 5(b)—color coded in orange and purple. It becomes evident that both states do not exhibit any out-of-plane spin polarization. This is a consequence of the effective sixfold symmetry of the real Re(0001) surface consisting of flat terraces with alternating A- and B-type surface terminations. Note that the spectra for the out-of-plane spin-polarization component are identical to the spin-averaged spectra for the Rashba-component [see spectra with black symbols at the bottom of Fig. 5(b) and as well in Fig. 1(b)]. This proves the consistent performance of our three-dimensional spin-polarization-detection system.

Figure 6 shows results from experimental and theoretical investigations for electronic states along $\overline{\Gamma}\,\overline{\mathrm{K}}$. Compared with Fig. 5(a), the ARPES measurement in Fig. 6(a) covers an extended $\mathbf{k}_\parallel$ range up to the $\overline{\mathrm{K}}$ point. The presentation of our theoretical results in Figs. 6(b) and 6(c) is the same as in Figs. 2 and 4, except for the marker size in Fig. 6(c), which is capped at high intensities for reasons of clarity.

Compared with Fig. 5(a), we find additional spectral features in Fig. 6(a), namely, ν, ξ, π, ρ, σ, and τ. Based on the DFT calculations shown in Fig. 6(b), we attribute these features to surface-derived states (σ and τ) and to band-gap

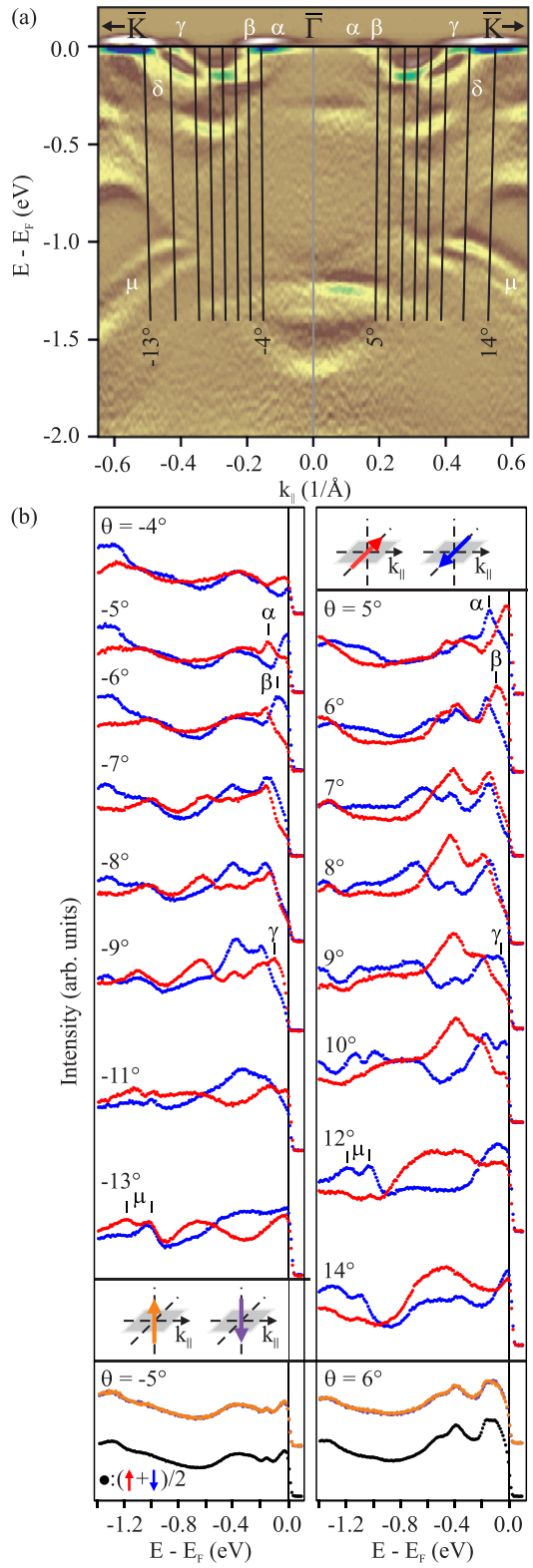

FIG. 5. (S)ARPES data for Re(0001) using *p*-polarized light of $\hbar\omega = 24$ eV. (a) Contour plot of ARPES intensity for $E(\mathbf{k}_\parallel)$ along $\overline{\Gamma}\,\overline{\mathrm{K}}$ (second derivative). (b) Spin-resolved spectra (Rashba component in red and blue, spin-averaged Rashba component in black, out-of-plane component in orange and purple) for selected electron emission angles θ [marked by black lines in panel (a)]. Note that orange markers were drawn on top of the purple ones. The Greek letters are used to label spectral features.

boundaries or regions of high bulk-band density (ν, ξ, π, and ρ).

In the following, we discuss the spin-resolved data of Fig. 5(b) together with DFT calculations in Figs. 6(b) and 6(c). The interpretation of the spin-polarized intensities of α, β, and γ along $\overline{\Gamma}\,\overline{\mathrm{K}}$ is equivalent to our discussion of the data along $\overline{\Gamma}\,\overline{\mathrm{M}}$: Lower spectral intensity of α compared with β, observed spin polarization of γ with reversed sign compared with intrinsic spin polarization. In contrast, the highly spin-polarized doublet feature δ along $\overline{\Gamma}\,\overline{\mathrm{M}}$ is observed as a weakly spin-polarized broad feature along $\overline{\Gamma}\,\overline{\mathrm{K}}$.

Finally, regarding μ, the doublet is intrinsically spin polarized, spin-up (spin-down) in the component with higher (lower) binding energy for negative $\mathbf{k}_\parallel$ and vice versa for positive $\mathbf{k}_\parallel$ [see Fig. 6(b)]. The situation changes for the component with lower binding energy when including transitions into final states, as shown in Fig. 6(c). Here, the dominant spin channel changes as a function of $\mathbf{k}_\parallel$. In agreement with this prediction, for this $\mathbf{k}_\parallel$ range, the SARPES spectra in Fig. 5(b) show intensities in both spin channels ($11^\circ < |\theta| < 14^\circ$). Moreover, the measured spin polarization of the component with higher binding energy matches the prediction of an almost complete spin polarization.

C. Rashba parameter of the W-shaped surface state

In the following, we aim to quantify the strength of SOC on Re(0001) by investigating the spin splitting of the W-shaped state. So far, "a Rashba splitting of 0.4 Å^{-1}" is reported for the surface state of Re(0001) [11]. We assume that this value describes the momentum offset of the two free-electron-like bands for the two opposite spin directions. It is not reported, however, how this surprisingly large value was derived from the data. In the case of simple parabolic E vs $\mathbf{k}_\parallel$ dispersion, the momentum offset is independent of energy. For the surface state of Re(0001) we find that the offset ranges between 0.05 Å^{-1} at E_F and 0.07 Å^{-1} at $E - E_\mathrm{F} = -50$ meV, in good agreement with our calculations (see Figs. 2 and 6).

According to the Rashba model, usually, the quantitative measure of the SOC is given by the Rashba parameter α_R, which is defined as

$$E_\pm(\mathbf{k}_\parallel) = \hbar^2\mathbf{k}_\parallel^2/2m^* \pm \alpha_\mathrm{R}|\mathbf{k}_\parallel|$$

for a free-electron-like state with m^* denoting the effective mass [27]. The prototypical L-gap surface state of Au(111), for example, exhibits a Rashba parameter of 0.36 eV Å [1]. Since the atomic numbers of Re and Au differ only by four, we expect a similar influence of SOC on the surface states and, therefore, their Rashba parameters should be comparable.

In our analysis of the spin splitting between α and β, we are faced with two limitations. Around $\overline{\Gamma}$, the W-shaped state is located above E_F and, therefore, inaccessible to ARPES. Furthermore, for $|\mathbf{k}_\parallel| > 0.2$ Å^{-1}, hybridization causes deviations from an almost parabolic energy dispersion. As a consequence, we determined the energetic positions of α and β and their energy splitting $\Delta E_{\alpha\beta}$ from EDCs in a rather small $\mathbf{k}_\parallel$ range.

Our findings are presented in Fig. 7. Figures 7(a) and 7(c) show the ARPES intensities for $\overline{\Gamma}\,\overline{\mathrm{M}}$ and $\overline{\Gamma}\,\overline{\mathrm{K}}$, respectively, as contour plots for *p*-polarized photons of $\hbar\omega = 24$ eV in

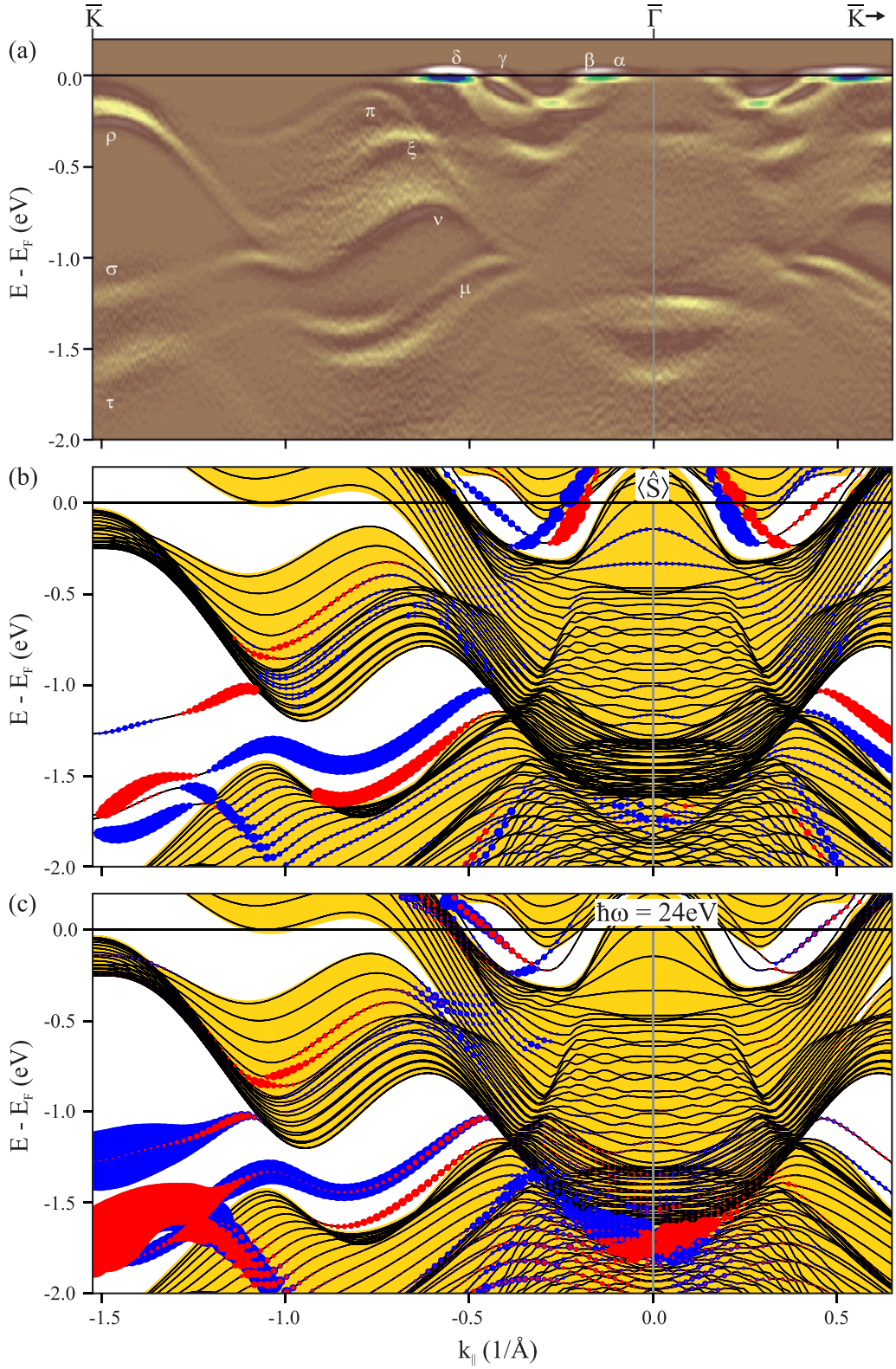

FIG. 6. Experimental and theoretical results for Re(0001) along $\overline{\Gamma}\,\overline{\mathrm{K}}$. (a) Contour plot of ARPES intensity (second derivative). The data displayed here consist of three measurements for a limited $\mathbf{k}_\parallel$ range, which are stitched together. (b), (c) DFT calculations for the same energy and $\mathbf{k}_\parallel$ ranges. The surface-projected bulk band structure is indicated by golden-shaded areas. Red (blue) dots in panel (b) indicate the intrinsic spin expectation value $\langle\hat{S}\rangle$ regarding the Rashba component for spin-up (spin-down) electrons of the surface states. (c) Calculations including transition matrix elements using free-electron-like final states and $\hbar\omega = 24$ eV. The dot size is a measure of the expected spectral intensity in the SARPES experiment. Note that the marker size was capped for reasons of clarity, which comes into effect for $\mathbf{k}_\parallel < -1.0$ Å^{-1}.

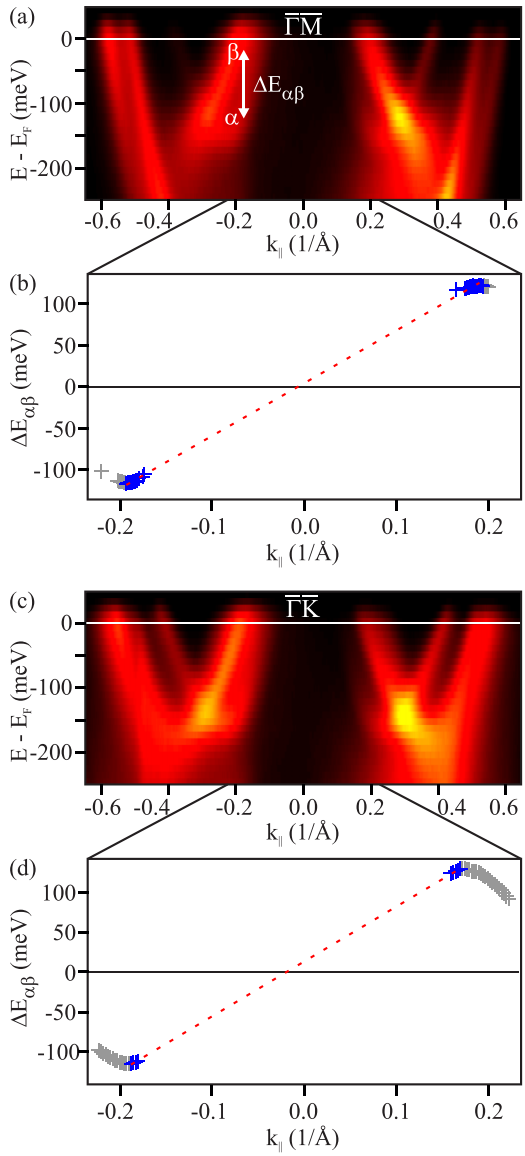

FIG. 7. Determination of the Rashba parameter α_R from ARPES data using *p*-polarized light and $\hbar\omega = 24$ eV. (a), (c) Contour plot of ARPES intensity for $\overline{\Gamma}\,\overline{M}$ and $\overline{\Gamma}\,\overline{K}$. (b), (d) Extracted energy splittings $\Delta E_{\alpha\beta}$ as blue and gray symbols, plotted as a function of $\mathbf{k}_\parallel$. The red-dotted lines are linear fits to the blue data points.

a black-red-yellow color scale. The spin splittings $\Delta E_{\alpha\beta}$ for the respective directions, derived from EDCs, are displayed as blue and gray symbols in Figs. 7(b) and 7(d). We used gray symbols for $\mathbf{k}_\parallel$ regions where hybridization comes into play and deviations from the simple Rashba model are expected. The gradients of linear functions (red dotted lines), which are fit to the blue data points, yield $2\alpha_R$. For $\overline{\Gamma}\,\overline{M}$ and $\overline{\Gamma}\,\overline{K}$, we obtain $\alpha_R^{\overline{\Gamma}\overline{M}} = (0.32 \pm 0.01)$ eV Å and $\alpha_R^{\overline{\Gamma}\overline{K}} = (0.34 \pm 0.01)$ eV Å, respectively. The uncertainties of the results are estimated by varying the number of data points included in the fit procedure. The theoretical results yield similar values of 0.35 and 0.37 eV Å for $\overline{\Gamma}\,\overline{M}$ and $\overline{\Gamma}\,\overline{K}$, respectively. Interestingly, both experimental and theoretical results suggest a slight warping of the Rashba parameter α_R.

V. CONCLUSION

We presented a comprehensive experimental and theoretical investigation of the surface electronic structure of Re(0001). Experimentally, we used spin- and angle-resolved photoemission to measure the spin-dependent $E(\mathbf{k}_\parallel)$ dispersion of electronic states along the $\overline{\Gamma}\,\overline{M}$ and $\overline{\Gamma}\,\overline{K}$ directions. To interpret the data, we employed calculations based on density-functional theory, among them calculations including transitions into free-electron-like final states with the corresponding matrix elements. The theoretically predicted out-of-plane spin polarization was experimentally inaccessible due to monatomic steps of a real Re(0001) surface with alternating terminations. This leads to an effective sixfold surface symmetry. For the surface state around $\overline{\Gamma}$, we determined Rashba parameters α_R of 0.32 and 0.34 eV Å along $\overline{\Gamma}\,\overline{M}$ and $\overline{\Gamma}\,\overline{K}$, respectively—in good agreement with theoretical calculations. The slightly different values for the two directions suggest a slight warping of α_R. The Rashba parameters for the Re(0001) surface band are very similar to the corresponding value for the paradigmatic *L*-gap surface state of Au(111), which is 0.36 eV Å. As expected from the atomic numbers, the strength of SOC for Re(0001) and Au(111) appear comparable.

ACKNOWLEDGMENTS

M.D. and M.H. gratefully acknowledge the hospitality of the Hiroshima Synchrotron Radiation Center and the excellent experimental support. We thank Shiv Kumar and Pascal J. Grenz for their help with the measurements and Jürgen Braun and Jan Minár for fruitful discussions. (S)ARPES measurements were performed with the approval of the HiSOR program advisory committee (Proposals No. 19BG026 and No. 20AU006). This work was supported by JSPS KAKENHI Grants No. 16H02114, No. 18H01954, and No. 20H00347. We thank N-BARD, Hiroshima University, for supplying the liquid helium.

[1] S. LaShell, B. A. McDougall, and E. Jensen, Spin Splitting of an Au(111) Surface State Band Observed with Angle Resolved Photoelectron Spectroscopy, Phys. Rev. Lett. **77**, 3419 (1996).

[2] F. Reinert, G. Nicolay, S. Schmidt, D. Ehm, and S. Hüfner, Direct measurements of the *L*-gap surface states on the (111) face of noble metals by photoelectron spectroscopy, Phys. Rev. B **63**, 115415 (2001).

[3] M. Hoesch, M. Muntwiler, V. N. Petrov, M. Hengsberger, L. Patthey, M. Shi, M. Falub, T. Greber, and J. Osterwalder, Spin structure of the Shockley surface state on Au(111), Phys. Rev. B **69**, 241401(R) (2004).

[4] S. N. P. Wissing, C. Eibl, A. Zumbülte, A. B. Schmidt, J. Braun, J. Minár, H. Ebert, and M. Donath, Rashba-type spin splitting at Au(111) beyond the Fermi level: The other part of the story, New J. Phys. **15**, 105001 (2013).

[5] K. Miyamoto, A. Kimura, K. Kuroda, T. Okuda, K. Shimada, H. Namatame, M. Taniguchi, and M. Donath, Spin-Polarized Dirac-Cone-Like Surface State with *d* Character at W(110), Phys. Rev. Lett. **108**, 066808 (2012).

[6] H. Mirhosseini, M. Flieger, and J. Henk, Dirac-cone-like surface state in W(110): Dispersion, spin texture and photoemission from first principles, New J. Phys. **15**, 033019 (2013).

[7] L. F. Mattheiss, Band structure and Fermi surface for rhenium, Phys. Rev. **151**, 450 (1966).

[8] A. Urru and A. Dal Corso, Spin-polarized electronic surface states of Re(0001): An *ab initio* investigation, Surf. Sci. **686**, 22 (2019).

[9] B. S. Mun, C. Lee, V. Stamenkovic, N. M. Markovic, and P. N. Ross, Jr., Electronic structure of Pd thin films on Re(0001) studied by high-resolution core-level and valence-band photoemission, Phys. Rev. B **71**, 115420 (2005).

[10] S. Ouazi, T. Pohlmann, A. Kubetzka, K. von Bergmann, and R. Wiesendanger, Scanning tunneling microscopy study of Fe, Co and Cr growth on Re(0001), Surf. Sci. **630**, 280 (2014).

[11] H. J. Elmers, J. Regel, T. Mashoff, J. Braun, S. Babenkov, S. Chernov, O. Fedchenko, K. Medjanik, D. Vasilyev, J. Minár, H. Ebert, and G. Schönhense, Rashba splitting of the Tamm surface state on Re(0001) observed by spin-resolved photoemission and scanning tunneling spectroscopy, Phys. Rev. Res. **2**, 013296 (2020).

[12] J. Regel, T. Mashoff, and H. J. Elmers, Quasiparticle interference of spin momentum locked surface states at step edges on Re(0001), Phys. Rev. B **102**, 115404 (2020).

[13] S. Schemmelmann, P. Krüger, F. Schöttke, and M. Donath, Rashba-split surface state and spin-dependent photon emission from Re(0001) at $\overline{\Gamma}$, Phys. Rev. B **104**, 205425 (2021).

[14] F. Schöttke, S. Schemmelmann, P. Krüger, and M. Donath, Rashba-split image-potential state and unoccupied surface electronic structure of Re(0001), Phys. Rev. B **105**, 155419 (2022).

[15] M. Holtmann, P. Krüger, K. Miyamoto, T. Okuda, P. J. Grenz, S. Kumar, K. Shimada, and M. Donath, Distinct Tamm and Shockley surface states on Re(0001) mixed by spin-orbit interaction, Phys. Rev. B **105**, L241412 (2022).

[16] See Supplemental Material at http://link.aps.org/supplemental/10.1103/PhysRevB.107.165420 for photon-energy-dependent ARPES results for the electronic states in $\overline{\Gamma}\,\overline{\mathrm{M}}$ direction.

[17] T. Okuda, K. Miyamaoto, H. Miyahara, K. Kuroda, A. Kimura, H. Namatame, and M. Taniguchi, Efficient spin resolved spectroscopy observation machine at Hiroshima Synchrotron Radiation Center, Rev. Sci. Instrum. **82**, 103302 (2011).

[18] T. Okuda, K. Miyamoto, A. Kimura, H. Namatame, and M. Taniguchi, A double VLEED spin detector for high-resolution three dimensional spin vectorial analysis of anisotropic Rashba spin splitting, J. Electron Spectrosc. Relat. Phenom. **201**, 23 (2015).

[19] R. D. Diehl, J. Ledieu, N. Ferralis, A. W. Szmodis, and R. McGrath, Low-energy electron diffraction from quasicrystal surfaces, J. Phys.: Condens. Matter **15**, R63(R) (2003).

[20] J. P. Perdew and A. Zunger, Self-interaction correction to density-functional approximations for many-electron systems, Phys. Rev. B **23**, 5048 (1981).

[21] D. R. Hamann, Generalized norm-conserving pseudopotentials, Phys. Rev. B **40**, 2980 (1989).

[22] L. Kleinman and D. M. Bylander, Efficacious Form for Model Pseudopotentials, Phys. Rev. Lett. **48**, 1425 (1982).

[23] B. Stärk, P. Krüger, and J. Pollmann, Magnetic anisotropy of thin Co and Ni films on diamond surfaces, Phys. Rev. B **84**, 195316 (2011).

[24] L. A. Hemstreet, C. Y. Fong, and J. S. Nelson, First-principles calculations of spin-orbit splittings in solids using nonlocal separable pseudopotentials, Phys. Rev. B **47**, 4238 (1993).

[25] H. J. Monkhorst and J. D. Pack, Special points for Brillouin-zone integrations, Phys. Rev. B **13**, 5188 (1976).

[26] S. N. P. Wissing, A. B. Schmidt, H. Mirhosseini, J. Henk, C. R. Ast, and M. Donath, Ambiguity of Experimental Spin Information from States with Mixed Orbital Symmetries, Phys. Rev. Lett. **113**, 116402 (2014).

[27] Y. A. Bychkov and E. I. Rashba, Properties of a 2D electron gas with lifted spectral degeneracy, Pis'ma Zh. Eksp. Teor. Fiz **39**, 66 (1984) [JETP Lett. **39**, 78 (1984)].